PRT6/At5g02310 encodes an *Arabidopsis* ubiquitin ligase of the N-end rule pathway with arginine specificity and is not the *CER3* locus

Marcus Garzón[a], Karolin Eifler[a], Andrea Faust[b], Hartmut Scheel[c], Kay Hofmann[c], Csaba Koncz[a], Alexander Yephremov[b], Andreas Bachmair[a,*]

[a] *Department of Plant Developmental Biology, Max Planck Institute for Plant Breeding Research, Carl-von-Linné-Weg 10, D-50829 Cologne, Germany*
[b] *Department of Molecular Plant Genetics, Max Planck Institute for Plant Breeding Research, Carl-von-Linné-Weg 10, D-50829 Cologne, Germany*
[c] *Bioinformatics Group, Miltenyi Biotec GmbH, Stockheimer Weg 1, D-50829 Cologne, Germany*

Abstract The eukaryotic N-end rule pathway mediates ubiquitin- and proteasome-dependent turnover of proteins with a bulky amino-terminal residue. *Arabidopsis* locus At5g02310 shows significant similarity to the yeast N-end rule ligase Ubr1. We demonstrate that At5g02310 is a ubiquitin ligase and mediates degradation of proteins with amino-terminal Arg residue. Unlike Ubr1, the *Arabidopsis* protein does not participate in degradation of proteins with amino-terminal Phe or Leu. This modified target specificity coincides with characteristic differences in domain structure. In contrast to previous publications, our data indicate that At5g02310 is not identical to *CER3*, a gene involved in establishment of a protective surface wax layer. At5g02310 has therefore been re-designated *PROTEOLYSIS 6* (*PRT6*), in accordance with its ubiquitin ligase function.
© 2007 Federation of European Biochemical Societies. Published by Elsevier B.V. All rights reserved.

Keywords: CER3; N-end rule; Ubiquitin; Wax biosynthesis; *Arabidopsis*

1. Introduction

Ubiquitin, a highly conserved 76 amino acid polypeptide, can be covalently linked to other proteins by enzymatic cascades consisting of ubiquitin activating and conjugating enzymes (UBA or E1, and UBC or E2, respectively), and of ubiquitin protein ligases (E3). Ubiquitin conjugation often leads to rapid degradation of substrate proteins by the large protease complex proteasome. Ubiquitin ligases are instrumental in substrate selection, and usually catalyze the linkage of ubiquitin's carboxyl-terminal Gly residue to ε-amino groups of internal Lys residues in substrates (for reviews, see [1–7]). Domains within the ligases serve for substrate binding, and therefore display sequence diversity. Similar diversity is found in the domains of substrate proteins that mediate association with ubiquitin ligases. The first degradation signal (degron) identified was a bulky amino-terminal residue of a protein [8]. The resulting set of degrons was termed the N-degrons [9,10]. In contrast, amino acids with small side chains such as Ala or Ser, which are frequently present at the amino ter-

mini of cellular proteins, do not target these proteins for degradation. Substrates of the eukaryotic N-end rule pathway include components of NO signaling in animals [11], and proteins important for pathogen defense and senescence in plants [12,13].

Saccharomyces cerevisiae was found to have a single ubiquitin ligase devoted to the N-end rule, termed Ubr1 [14], whereas mammals have several isoforms encoded by distinct genes [15]. A previous screen in *Arabidopsis* identified genes *PRT1–5* (*PROTEOLYSIS 1–5*) as potential components of the plant N-end rule pathway [16]. PRT1 was subsequently demonstrated to function as a ubiquitin ligase of the plant N-end rule pathway, but its restricted substrate specificity strongly suggested the existence of additional N-end rule ligases in plants [17,18].

In this work, we investigated the function of locus At5g02310, which encodes the *Arabidopsis* protein most similar to yeast N-end rule ligase Ubr1. Previous studies annotated this locus as *ECERIFERUM 3* (*CER3*), a gene essential for epicuticular wax biosynthesis [19,20]. *cer* mutants [21] are most easily identified by the glossy green color of their stems, because they lack the whitish layer of protective surface wax crystals. Numerous genes that are required for wax biosynthesis and transport have been identified (for recent reviews, see [22,23]). Based on these data, it appeared that At5g02310/ *CER3* could provide a link between the N-end rule pathway of protein degradation and wax biosynthesis or transport. We show that At5g02310 codes for a functional ubiquitin ligase of the N-end rule pathway of protein degradation. However, in contrast to previous claims, null mutations in this gene have a normal wax layer, implying that it is not the *CER3* locus. Consistent with previous designations in the *Arabidopsis* N-end rule pathway, At5g02310 was renamed *PRT6* (*PROTEOLYSIS 6*).

2. Materials and methods

2.1. Plant growth and genotyping
Plants were grown on soil under standard greenhouse long day conditions, with 16 h light/8 h dark cycles. Young plantlets were germinated on agar plates containing MS salts and 1% sucrose. Plant transformation of Col-0 accession was done by the floral dip method. The original *cer3* mutant seeds (line N33) were obtained from the Nottingham *Arabidopsis* Stock Centre. T-DNA insertion allele *prt6-1* was a kind gift of Syngenta Inc. (SAIL 1278_H11; Ref. [24]). The *prt6-1* insertion was detected by PCR, using oligonucleotides Garlic LB1

(GCC TTT TCA GAA ATG GAT AAA TAG CCT TGC TTC C) and ubrdn3 (GTT TCT TGT TCT GGG GAG GAT GGT TT) and LA Taq polymerase (TaKaRa). Similar PCR conditions, but with primers ubrdn3 and ubrup3 (AGG ACA ATA GGT ACA TAC TCA TTT GTT), served to detect wild-type sequence at the *prt6-1* T-DNA insertion site. T-DNA insertion allele *prt6-2* was identified in the GABI-KAT collection (GK270G04; Ref. [25]). The insertion was monitored using primers o8760 (GGG CTA CAC TGA ATT GGT AGC TC) and CER3up (CAA TGC AAA TCT GCG CAC AGA GAC T). Wild-type sequence at the *prt6-2* insertion site was monitored by PCR with oligonucleotides CER3up and CER3dn (TCC CTC TGC CAT GAC CCA GAT TC) and LA Taq polymerase (TaKaRa). Both *prt6* alleles were backcrossed several times to wild-type (Col-0). Calculation of map distance between *cer3* and *prt6-2* used the formulae $N(2r - r^2)/4$ for relative frequency of plants with (sulfadiazine resistance conferring) T-DNA insert in *PRT6* and *cer3* mutant phenotype, and $N(3 - 2r - r^2)/4$ to assess sulfadiazine-resistant plants with *CER3* (WT) phenotype. *r* is the frequency of recombination between the two loci, and *N* the total number of individuals analyzed (see Section 3).

2.2. DNA constructs

A fragment of pUPR vectors [18], containing the Gly$_n$-lacI extension, was amplified by PCR and linked to a fragment encoding a triple HA epitope tag. The sequence was cloned into pSK vector and extended by inserting a GUS cassette from vector pRT104GUS (a kind gift of R. Töpfer) to obtain vector pSKlacIHAGUS. The lacIHAGUS insert from this vector was inserted between Bgl II and Xba I sites of vectors pUPR-X (Ref. [18]; X denotes the amino acids Met, Arg, Leu, or Phe) to generate fusions of the stable reference protein DHFR-HA-ub with the X-lacI-3HA-GUS test proteins (called pUPR-GUS-X). Details of cloning, and sequences of the constructs, can be provided upon request. Xho I Xba I fragments from vectors pUPR-GUS-X were inserted into plant binary vector p3 [26]. The constructs, called p3GUS-X, were used for plant transformation and allow expression of the inserted ORF under control of a triple CaMV 35S promoter. The ensuing protein products are referred to as X-GUS (X being the single letter code for the amino acid exposed after cleavage of the translation product by ubiquitin-specific proteases).

2.3. GUS staining

Staining of plants to visualize GUS activity was carried out as described [27].

2.4. Western blotting

Leaf extracts were prepared and separated on polyacrylamide gels as described [18]. The gel was further processed as recommended for fluorescence detection (Odyssey Li-Cor), starting with protein transfer onto BA85 nitrocellulose membranes (Whatman). After saturation of residual protein binding sites (Odyssey blocking buffer; Li-Cor), the blot was incubated with rat anti-HA antibody (Roche), followed by IRdye 800-conjugated goat anti-rat IgG secondary antibody (Rockland). The Odyssey Infrared Imager (Li-Cor) was used for band detection and quantification with an excitation wavelength of 780 nm, to record emission at 820 nm.

2.5. Wax analysis

Procedures used for GC–MS analysis of cuticular wax composition have been described previously [28].

2.6. Bioinformatic analysis

Sequence database searches were performed by BLAST [29], and by generalized profile method [30]. Multiple sequence alignments were calculated by the MUSCLE program [31].

3. Results

Sequence analysis of potential *Arabidopsis* ubiquitin ligases revealed that gene At5g02310 shows significant similarity to the yeast ubiquitin ligase gene *UBR1*. As At5g02310 has been reported earlier to encode ECERIFERUM 3 (CER3), specify-

ing an important function in wax biosynthesis, it appeared interesting to examine the possible ubiquitin ligase activity of the At5g02310 gene product. Revisiting the details of *CER3* cloning by Hannoufa et al. [19], we noticed that the available data, for instance regarding chromosomal location of *CER3*, were not fully consistent. The wax-deficient *cer3* mutant was first identified by Koornneef et al. (Ref. [21]; allele *cer3-1*), and mapped to the bottom arm of chromosome 5. Hannoufa et al. [19] described an allele inducted by T-DNA insertional mutagenesis, and reported that the T-DNA insertion was localized in the untranslated 3′ terminal portion of an open reading frame (ORF). A standard set of experiments, including mutant complementation by a fragment of genomic DNA, led the authors to propose that this ORF is the *CER3* gene, which was accordingly deposited in the EMBL database (EMBL accession number X95962). Completion of the chromosome 5 sequence revealed that X95962, corresponding to the At5g02310 gene, is in fact located on the top arm of chromosome 5, far away from the previously determined position of the *cer3-1* mutation [21,32]. Gene prediction models further suggested that At5g02310, and the adjacent ORF At5g02300, encode a single protein, showing sequence similarity to yeast Ubr1 (Fig. 1). Current annotation (GenBank accession number NP_195851) therefore lists this larger ORF as a single transcription unit, using designation At5g02310. Based on the report of Hannoufa et al. [19], At5g02310 was annotated by genome curators as the ubiquitin-protein ligase *CER3* required for wax biosynthesis, notwithstanding the fact that the fragment used in Ref. [19] for the complementation of a *cer3* mutant did not contain the complete At5g02310 gene.

Homologous sequence segments between At5g02310 and yeast *UBR1* extend across the entire ORF, indicating that the proteins could perform a similar function (Fig. 1B, and Supplementary Figure). For this reason, and for reasons described in detail in the following, we used abbreviation *PRT6* (*PR*OT*E*OLYSIS 6) instead of *CER3* to designate At5g02310. Ubr1 is the ubiquitin ligase of the yeast N-end rule pathway of protein degradation [14] (see also Section 1). It was previously shown that the N-end rule pathway exists in plants [13,16,33,34], and a function for PRT6 in the plant N-end rule pathway was tested using loss-of-function mutants, and model substrates.

In view of possible ambiguity regarding the *CER3* locus, T-DNA insertion lines with defined sites of integration within At5g02310 were obtained from the SAIL and GABI-KAT collections. Characterization of these T-DNA tagged mutants showed that the SAIL 1278_H11 (*prt6-1*) mutant carried an insertion in sequences originally annotated as At5g02300, interrupting *PRT6* close to the 5′ end (Fig. 1A). In the GABI-KAT GK270G04 (*prt6-2*) mutant, the T-DNA insertion interrupted the genomic DNA fragment that was originally used for *cer3* complementation in Ref. [19]. Much to our surprise, homozygous plants carrying either the *prt6-1*, or the *prt6-2* mutant allele failed to display visually an *eceriferum* phenotype.

To further investigate the discrepancy to previously published genetic data of the *CER3* locus, we compared the phenotypes of homozygous T-DNA insertion mutants with the original *cer3-1* allele. Because *cer3-1* was generated in L*er* background, whereas the *prt6-1* and *prt6-2* mutations were in the Col-0 background, we performed *prt6-1* × *cer3-1* and *prt6-2* × *cer3-1* crosses along with a control cross Col-0
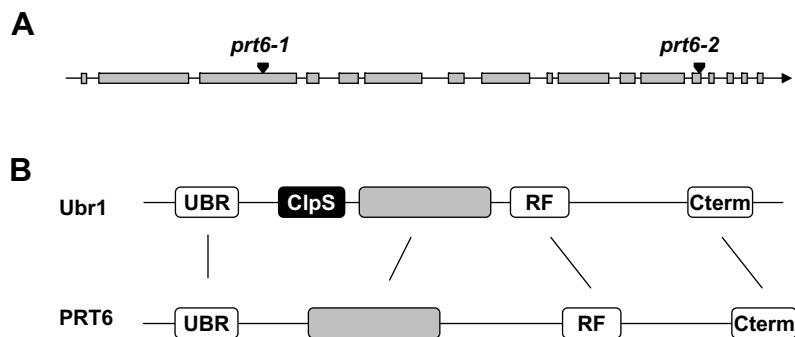
Fig. 1. The gene *PRT6*/At5g02310 (formerly *CER3*). (A) Structure of the transcribed region. Blocks represent parts of the open reading frame. Arrowheads indicate positions of T-DNA insertions in mutant alleles *prt6-1* and *prt6-2*. (B) Schematic alignment of protein domains of PRT6 and its yeast sequelog, Ubr1. Sequence blocks with particularly high conservation are indicated as thick bars. UBR, UBR domain; ClpS, region with similarity to *Escherichia coli* ClpS; RF, region containing a RING finger motif; C-term, carboxyl-terminal similarity region. A sequence alignment that formed the basis for these assignments is available as Supplementary material.

(wild-type) × *cer3-1*. When performing these complementation tests, we also reasoned that, if any of the *prt* or *cer* alleles would result in a leaky or semi-dominant phenotype, the hemizygous state would be most sensitive in revealing such more subtle deviations from wild-type. Koorneef et al. [21] demonstrated that the *cer3-1* allele is recessive, and as expected, F1 plants from the cross Col-0 × *cer3-1* were visually wild-type, and were readily distinguishable by eye from *cer3-1*. Whereas *cer3-1* plants had darker, iridescent green stems and were almost completely sterile under the intermediate humidity conditions of our greenhouses, F1 hybrids were fully fertile and had a whitish stem color due to a wax coating. F1 hybrids from the two other crosses, *prt6-1* × *cer3-1* and *prt6-2* × *cer3-1*, were indistinguishable from Col-0 × *cer3-1* progeny. The presence of these T-DNA insertions in the F1 hybrids was confirmed by PCR (data not shown). We thus conclude that *prt6* and *cer3-1* are not allelic.

As *cer3* mutants accumulate significantly lower levels of wax in both stems and leaves [35], the *cer3-1*, *prt6-1* and *prt6-2* mutants, and all F1 hybrids were subjected to leaf wax analysis (Table 1). The amount of compounds from the sterol family (cholesterol, campesterol) was similar in all genotypes, and served as a control. Likewise, C26 alcohol and C28 alcohol content was not decreased in *cer3-1* mutants compared to wild-type and the *prt6* mutants. In contrast, the amounts of alkanes with chain length 29 or higher, alcohols with chain length 30 or 32, and fatty acids with chain length 30 or 32 were at least 10-fold reduced in the *cer3-1* mutant compared to *prt6* mutants. The observed values of wax constituents in *cer3-1* and *prt6* mutants were in good agreement with published data for *cer3* and wild-type plants, respectively [35,36]. Our conclusion that *PRT6* is not allelic to *CER3* was also supported by the fact that all F1 plants had comparable lipid content (Table 1). In all those cases where the abundance of a lipid constituent was significantly reduced in the *cer3-1* mutant, we observed a reduction of up to 50% in the F1 hybrids compared to *prt6* mutant lines. This finding indicated a gene dose effect, i.e. 50% *CER3* gene dose in the F1 plants resulted in approximately 50% abundance of those lipid compounds that depended on *CER3* gene activity. Because all F1 plants had the same Ler–Col-0 genetic background, we concluded that *prt6* mutant plants contained an intact copy of the *CER3* gene.

To determine the genetic distance between *CER3* and the At5g02310 locus, we analyzed F2 selfed progeny of the *cer3-1* × *prt6-2* cross. For linkage analysis, we took advantage of the *sul* gene encoded by the *prt6-2* T-DNA insertion. This allowed for efficient selection of sulfadiazine-resistant plants. If *CER3* and At5g02310 were closely linked, no *cer3* plants resistant to the antibiotic would be expected in the F2 generation. Altogether, 313 plants survived sulfadiazine selection, and 62 of these displayed the *cer3* phenotype, while 251 were wild-type. As detailed in 2.1, recombination between loci At5g02310 and *CER3* occurred with frequency 33% ($r = 0.330$), suggesting that *CER3* is on chromosome 5, but maps at quite a distance from At5g02310. This result is in good agreement with the original mapping by Koornneef et al. [21], who determined that *cer3* maps to the bottom arm of chromosome 5. To further substantiate the conclusion that *PRT6* (At5g02310) and *CER3* genes are therefore not allelic, we resequenced the *PRT6* gene in the *cer3-1* mutant N33 line and found no mutations compared to the Ler parent (data not shown).

To determine the possible involvement of PRT6 in the *Arabidopsis* N-end rule pathway, we used model ubiquitylation substrates. Table 2 summarizes the known enzymology of the plant N-end rule pathway, including data presented below. Our assays were based on the ubiquitin fusion degradation technique. This method allows assessment of the metabolic stability of a test protein by comparison to a metabolically stable reference protein that is co-translated with, but cleaved from the test protein after synthesis (Fig. 2). Cleavage is carried out by ubiquitin-specific intracellular proteases that recognize the ubiquitin moiety present at the carboxyl end of the reference protein. This method, developed by Varshavsky and co-workers [37,38], was previously applied in different variations in plants [18,39]. *prt6-1* plants were crossed to transgenic lines harboring N-end rule test substrates (Fig. 2). As a control, we included the previously characterized *prt1* mutation in these experiments. As indicated in Table 2, our previous studies suggested that ubiquitin ligase PRT6 would not mediate turnover of N-end rule substrates with an aromatic first amino acid residue, because these are substrates of PRT1 [18]. We expected that if PRT6 functions as ubiquitin ligase, the substrates should either start with basic amino termini (represented by Arg in this investigation) or with aliphatic hydrophobic residues such as Leu. In contrast to that, the yeast PRT6 sequelog, Ubr1, has two distinct binding sites for destabilizing amino termini, one for basic residues and one for (aliphatic and

Table 1
Plants with mutations in At5g02310 have normal wax content

Lipid constituent	Genotype[a]	Quantity[b] ($\mu g/cm^2$ leaf area)
Cholesterol	cer3-1	0.019 ± 0.004
	prt6-1	0.023 ± 0.003
	prt6-2	0.031 ± 0.004
	F1 Col-0 × cer3-1	0.025 ± 0.004
	F1 prt6-1 × cer3-1	0.029 ± 0.001
	F1 prt6-2 × cer3-1	0.029 ± 0.001
Campesterol	cer3-1	0.041 ± 0.005
	prt6-1	0.048 ± 0.003
	prt6-2	0.050 ± 0.005
	F1 Col-0 × cer3-1	0.040 ± 0.004
	F1 prt6-1 × cer3-1	0.028 ± 0.001
	F1 prt6-2 × cer3-1	0.039 ± 0.011
C29 alkane	cer3-1	0.012 ± 0.002
	prt6-1	0.160 ± 0.005
	prt6-2	0.205 ± 0.028
	F1 Col-0 × cer3-1	0.076 ± 0.005
	F1 prt6-1 × cer3-1	0.112 ± 0.005
	F1 prt6-2 × cer3-1	0.131 ± 0.008
C31 alkane	cer3-1	Below det. level
	prt6-1	0.219 ± 0.013
	prt6-2	0.293 ± 0.047
	F1 Col-0 × cer3-1	0.130 ± 0.002
	F1 prt6-1 × cer3-1	0.163 ± 0.010
	F1 prt6-2 × cer3-1	0.153 ± 0.025
C33 alkane	cer3-1	Below det. level
	prt6-1	0.051 ± 0.001
	prt6-2	0.053 ± 0.009
	F1 Col-0 × cer3-1	0.022 ± 0.002
	F1 prt6-1 × cer3-1	0.021 ± 0.001
	F1 prt6-2 × cer3-1	0.020 ± 0.005
C26 alcohol	cer3-1	0.024 ± 0.002
	prt6-1	0.016 ± 0.002
	prt6-2	0.022 ± 0.005
	F1 Col-0 × cer3-1	0.013 ± 0.002
	F1 prt6-1 × cer3-1	0.022 ± 0.002
	F1 prt6-2 × cer3-1	0.018 ± 0.001
C28 alcohol	cer3-1	0.032 ± 0.004
	prt6-1	0.036 ± 0.004
	prt6-2	0.047 ± 0.011
	F1 Col-0 × cer3-1	0.024 ± 0.002
	F1 prt6-1 × cer3-1	0.039 ± 0.004
	F1 prt6-2 × cer3-1	0.027 ± 0.005
C30 alcohol	cer3-1	0.003 ± 0.001
	prt6-1	0.028 ± 0.000
	prt6-2	0.084 ± 0.017
	F1 Col-0 × cer3-1	0.018 ± 0.004
	F1 prt6-1 × cer3-1	0.013 ± 0.001
	F1 prt6-2 × cer3-1	0.012 ± 0.001
C32 alcohol	cer3-1	Below det. level
	prt6-1	0.127 ± 0.006
	prt6-2	0.169 ± 0.018
	F1 Col-0 × cer3-1	0.096 ± 0.005
	F1 prt6-1 × cer3-1	0.068 ± 0.001
	F1 prt6-2 × cer3-1	0.108 ± 0.007
C30 acid	cer3-1	Below det. level
	prt6-1	0.014 ± 0.003
	prt6-2	0.032 ± 0.001
	F1 Col-0 × cer3-1	0.016 ± 0.004
	F1 prt6-1 × cer3-1	0.012 ± 0.001
	F1 prt6-2 × cer3-1	0.028 ± 0.006

Table 1 (*continued*)

Lipid constituent	Genotype[a]	Quantity[b] ($\mu g/cm^2$ leaf area)
C32 acid	cer3-1	0.005 ± 0.001
	prt6-1	0.090 ± 0.008
	prt6-2	0.082 ± 0.017
	F1 Col-0 × cer3-1	0.022 ± 0.003
	F1 prt6-1 × cer3-1	0.020 ± 0.001
	F1 prt6-2 × cer3-1	0.032 ± 0.004

[a]The *cer3-1* allele was in Ler background. All other mutations were in Col-0 background. The F1 hybrids therefore represent isogenic comparisons, devoid of variations due to different genetic background.
[b]Indicated are mean values of samples from three (in rare cases two) plants, ± standard error of the mean.

aromatic) hydrophobic residues [40,41]. Fig. 3 shows a histochemical staining assay, detecting substrate GUS proteins in different mutant backgrounds. In contrast to the stable M-GUS, the N-end rule substrates F-GUS, L-GUS and R-GUS were short-lived in wild-type plants. As expected, plants expressing F-GUS from a transgene accumulate this protein in the *prt1* background, so that plantlets stain blue with GUS enzyme substrate. The *prt6-1* mutation alters the degradation rate of R-GUS, but the mutation did not affect the turnover of F-GUS (an expected result), or L-GUS. Finally, plants harboring both *prt1* and *prt6-1* mutations showed accumulation of stable F-GUS and R-GUS substrates, but still degraded the L-GUS reporter construct. The results depicted in Fig. 3 thus suggested that PRT6 is a ubiquitin ligase of the N-end rule pathway specific for basic amino termini.

The accumulation of R-GUS protein in *prt6-1* mutants is genetically linked to the T-DNA insertion in *PRT6*. Ninety-one plantlets from an F2 population segregating for the *prt6-1* mutation and containing the R-GUS transgene were analyzed by GUS staining of leaves, and PCR-based genotyping. We found 100% co-segregation of the trait "GUS-positive staining" with homozygous T-DNA insertion at the *PRT6* locus. 26 of the 91 plants were GUS-positive and homozygous for the *prt6-1* T-DNA insertion, whereas the remaining 65 plants were GUS-negative and harbored at least one wild-type allele of the *PRT6* locus. From this result we concluded that the *prt6-1* allele is recessive and directly responsible for stabilization of the R-GUS test protein.

In order to obtain quantitative confirmation of the above described qualitative data (Fig. 3), another property of the N-end rule test constructs was exploited. The presence of influenza hemagglutinin (HA) tags allows immunological detection of both the GUS test protein and the co-translated, metabolically stable reference protein (Fig. 2). Protein extracts from different mutants were prepared, separated by SDS–PAGE, and subjected to Western blotting with anti-HA primary, and fluorescent dye-coupled secondary antibody. The dye conjugate used in these experiments permitted quantification of the HA epitope-containing proteins (Fig. 4A). Whereas extract from non-transformed plants gave a background of bands due to non-specific binding of the secondary antibody (or due to auto-fluorescence of some plant proteins), the gel regions containing reference protein (one asterisk) or the test protein (two asterisks) were almost devoid of such non-specific bands. Band intensity was quantitatively assessed by excitation and fluorescence detection. Fig. 4B shows that the measured values confirm the qualitative assays of Fig. 3. R-GUS protein

Table 2
The plant N-end rule pathway

Destabilizing residue	Ubiquitin ligase/transferase[a]	Gene identifier number	Reference
Arg, (Lys, His)[b]	PRT6	At5g02310	This work
Phe, Tyr, Trp	PRT1	At3g24800	[18]
Leu, (Ile)		?	
Asp, Glu, (ox. Cys)	DLS1[a]	At5g05700	[13]
(Asn, Gln)		?	

[a]Similarity considerations suggested that DLS1 (delayed leaf senescence 1)/AtATE1 is an aminoacyl-tRNA protein transferase, transferring Arg residues to extend the amino-terminal Asp or Glu.

[b]First amino acids that are destabilizing in animals or fungi, but were not directly tested for their destabilizing effect in plants, are shown in parentheses. Amino acid abbreviations are in standard three letter code; ox. Cys is Cysteine with SH group oxidized to give cysteic acid, which resembles Asp.
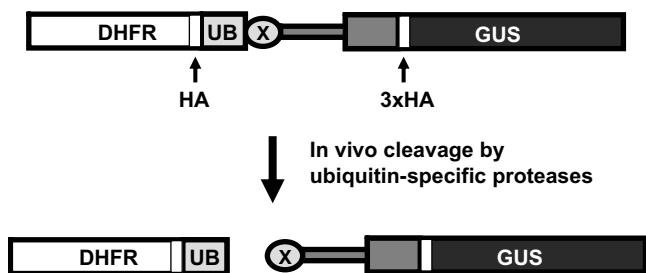

Fig. 2. Test constructs for plant N-end rule proteolysis assays. The stable, monomeric protein murine dihydrofolate reductase (DHFR, white) was fused to the amino terminus of ubiquitin (variant K48R; UB, light grey), followed by *Escherichia coli* beta glucuronidase (GUS, black). The GUS ORF was extended by unstructured amino acids (dark grey) to enhance the effect of destabilizing amino-terminal residues. During or briefly after translation, the fusion protein is cleaved into two parts by ubiquitin-specific proteases, a step that exposes variable amino acid X (light grey). HA epitopes allow immunological detection and quantitation of both cleavage products with the same antibody.

accumulated at least 10-fold higher in *prt6* plants compared to wild-type or *prt1* plants, and R-GUS levels approached the value obtained for the stable M-GUS construct. Because relative R-GUS abundance in the *prt6* mutant was still about 3-fold lower than M-GUS abundance in the wild-type, we could not rule out that another *Arabidopsis* ubiquitin ligase contributes to R-GUS turnover. In contrast, abundance of L-GUS substrate was not changed by the *prt6* mutation. Therefore, we concluded that *Arabidopsis* contains at least one more component of the N-end rule pathway, which is responsible for turnover of proteins with hydrophobic aliphatic amino termini, represented by L-GUS substrate in our assays.

4. Discussion

The N-end rule regulates a protein's half life according to its amino-terminal residue. Proteins with bulky first amino acids and unmodified amino-terminal amino groups are channeled into degradation pathways. In eukaryotes, degradation occurs via the ubiquitin proteasome system. In this work, we show that the gene product of At5g02310 is a sequelog of yeast N-end rule ligase Ubr1, and operates in degradation of N-end rule substrates with basic amino termini. We also show that previous reports stating that At5g02310 is the *CER3* gene are unsubstantiated. We therefore re-named the locus At5g02310 as *PRT6* (*PROTEOLYSIS 6*).
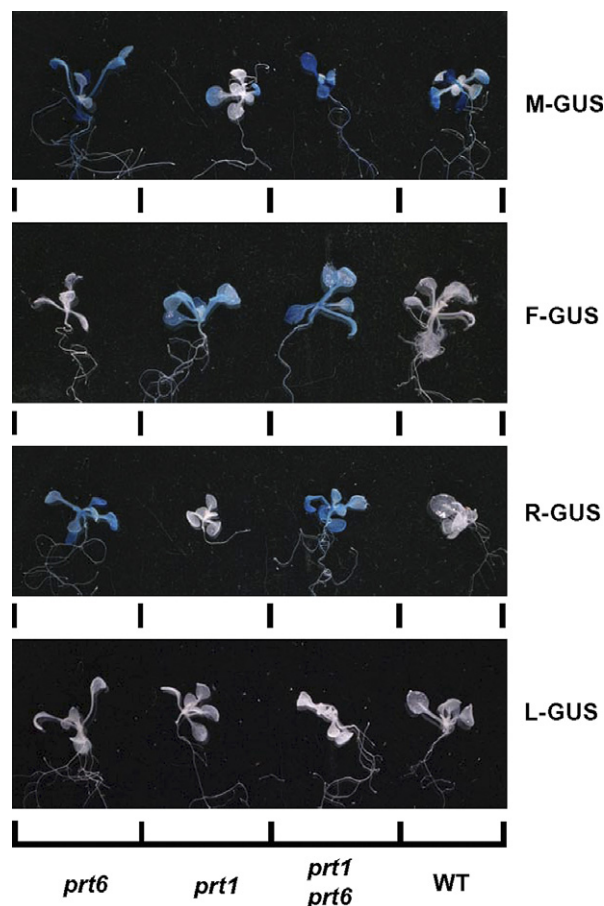

Fig. 3. Histochemical assay of GUS reporter protein in seedlings expressing ubiquitin fusion degradation test substrates (cf. Fig. 2). M-GUS, F-GUS, R-GUS, or L-GUS constructs were expressed in different genetic backgrounds, and plants were subsequently stained for GUS activity. Whereas M-GUS is stable in all genotypes, giving rise to blue coloration, F-GUS is stabilized only in presence of the *prt1* mutation, and R-GUS is stabilized in the *prt6* mutants. L-GUS abundance is unaffected by both mutations.

Arabidopsis PRT6 and yeast Ubr1 differ functionally in one important aspect. Whereas the yeast protein mediates turnover of proteins based on either hydrophobic, or basic amino termini, the plant protein has apparently lost its ability to mediate degradation of proteins with hydrophobic amino termini. This finding is in agreement with the existence of a second ubiquitin ligase in the plant N-end rule pathway, PRT1 (Table 2). The latter ubiquitin ligase, however, only mediates degradation of

A

B

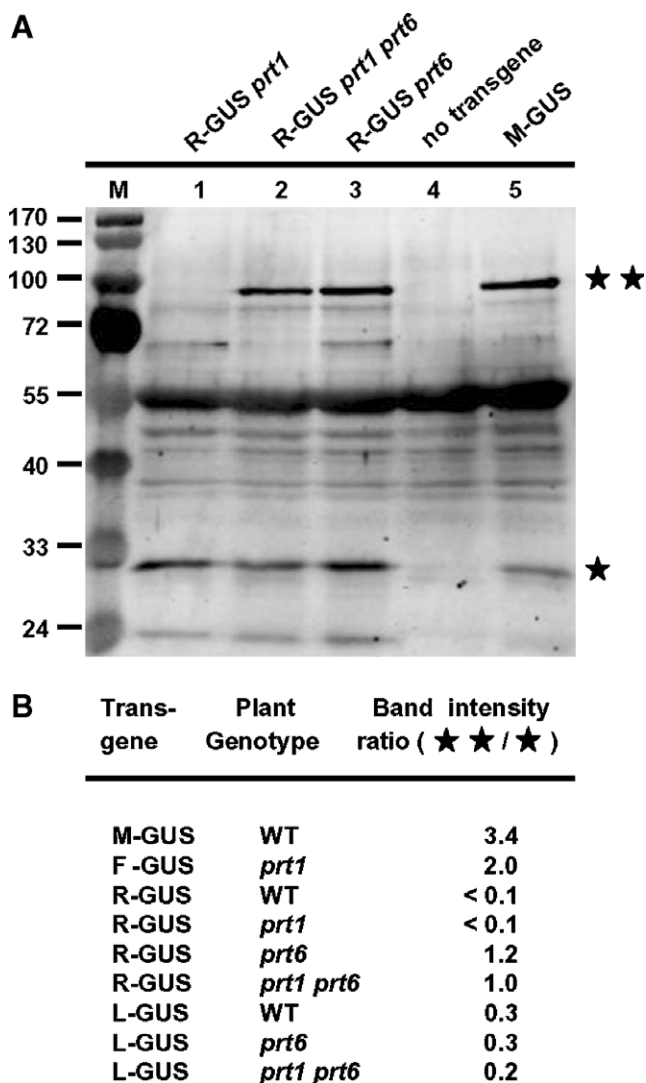| Trans-gene	Plant Genotype	Band intensity ratio (★★ / ★)
M-GUS	WT	3.4
F -GUS	prt1	2.0
R-GUS	WT	< 0.1
R-GUS	prt1	< 0.1
R-GUS	prt6	1.2
R-GUS	prt1 prt6	1.0
L-GUS	WT	0.3
L-GUS	prt6	0.3
L-GUS	prt1 prt6	0.2

Fig. 4. Detection and quantitative measurement of N-end rule substrates by protein blotting using fluorescent secondary antibody excitation. (A) Crude protein extracts from plants (genotypes listed above lanes) were separated by SDS–PAGE and transferred onto a membrane. Primary antibody incubation (anti-HA antibody) was followed by incubation with secondary antibody coupled to infrared fluorescent dye IR800. The processed blot was irradiated to record a fluorescence image. (1) Extract from *prt1* plants expressing R-GUS substrate. The *prt1* mutation does not affect degradation of R-GUS, as evidenced by the low intensity of the corresponding band. (2) Same as lane 1, but genotype *prt1 prt6*. (3) Same as lane 1, but plant genotype *prt6*. PRT6 mediates degradation of R-GUS, indicated by stabilization of R-GUS in its absence. (4) Extract from non-transgenic wild-type plant. (5) Extract from wild-type plant carrying the stable M-GUS control construct. Bands marked by one (stable reference protein – see Fig. 2) or two (GUS test protein) asterisks contain an HA epitope. Other bands correspond to cross-reacting proteins also present in plants carrying no transgene. (M) molecular mass markers (values in kDa to the left). (B) The ratio of fluorescence values for test versus reference protein in different transgene and genotype combinations were obtained from gels as shown in (A). The baseline value of ca. 3 for construct M-GUS results from the presence of three HA epitope tags on the test protein, versus one HA tag on the reference protein. Consistent with the visual assay of Fig. 3, R-GUS, but not L-GUS or F-GUS is stabilized in the *prt6* mutant background.

proteins with aromatic amino termini (Ref. [18]; Table 2). As a test protein with the aliphatic hydrophobic amino acid Leu at

its amino terminus is metabolically unstable in both single *prt1* and *prt6* mutants, and in the *prt1 prt6* double mutant (Figs. 3 and 4), we postulate the existence of at least one additional ubiquitin ligase in the plant N-end rule pathway.

It has been previously shown that basic and hydrophobic amino termini bind to different pockets on Ubr1 [40,41]. The so-called UBR domain is hypothesized to mediate interaction with basic amino termini. The proposed binding site for hydrophobic amino termini contains a region with similarity to bacterial ClpS protein. *Escherichia coli* ClpS can bind to proteins with hydrophobic amino-terminal residues and mediates their turnover in the (ubiquitin-independent) bacterial N-end rule pathway [42]. Interestingly, the inability of PRT6 to mediate degradation of proteins with hydrophobic amino termini correlates with poor conservation of this ClpS homology region (Fig. 1B and Supplementary Figure).

A recent report from Tasaki et al. [15] lists two additional proteins in *Arabidopsis* with UBR domain, At3g02260 and At4g23860. The former protein, designated *BIG* (*big* protein), is a regulator of auxin transport [43]. The latter, a sequelog of mammalian Ubr7, has no currently assigned name or function. The data presented in this work do not answer the question as to whether either of these two proteins operates in turnover of proteins with basic amino termini. We observed that the model substrate R-GUS (first amino acid Arg, see Fig. 2) is not completely stabilized in *prt6* mutants (Fig. 4). Residual instability in comparison to the proteolytically stable M-GUS may be due to conformational differences that make R-GUS a better substrate for other protein turnover pathways. Alternatively, the residual instability of R-GUS in *prt6* could be caused by active participation of BIG or At4g23860 in the plant N-end rule. The presence of a UBR domain in these two proteins certainly suggests that both can bind peptides with basic amino termini, but this does not necessarily imply that ubiquitylation is a consequence of binding. Yeast Ubr1, the founding member of UBR domain proteins, can bind large proteins with easily accessible basic amino-terminal residue, but the same pocket can bind short peptides as allosteric regulators [40,44]. This precedent leaves open the additional possibility that the function of UBR domains in either BIG or At4g23860 is the binding of regulatory peptides.

Our genetic and biochemical data clearly show that *PRT6* is not identical with the previously described *CER3* gene. Hannoufa et al. [19] presented the sequence X95962 (corresponding to the carboxyl-terminal half of PRT6) as the *CER3* gene, and work from the same group confirmed in a follow-up study that sequences of the 3' half of the *PRT6* gene can complement a *cer3* mutation [20]. However, the *cer3-1* mutation was mapped to the bottom arm of chromosome 5 [21], whereas *PRT6* is located at the top of this chromosome. *CER3* gene location was therefore an inconsistency between the genetic map and the genome sequencing data [32]. This inconsistency is now resolved, as *CER3* was incorrectly assigned to the At5g02310 locus. Simple visual inspection of homozygous *prt6* mutants indicated that mutant stems were covered by a normal wax layer, whereas the *cer3-1* mutant had drastically reduced surface wax. In addition, complementation tests between *prt6* and *cer3* mutations, as well as direct quantitative measurements of wax components, demonstrated that mutations in the At5g02310 (*PRT6*) gene cause no alteration in leaf wax composition. As interesting result related to regulation of wax production, we found an intermediate amount of long

chain wax constituents when there was heterozygosity at the *CER3* locus (Table 1). The biochemical data suggested that *CER3* is necessary to produce significant amounts of primary alcohols of chain length C30 or higher (but not for those with chain length C26 or C28), and to produce alkanes of chain length C29 or higher. Similarly, long chain fatty acids of chain length C30 and C32 were reduced more than 10-fold in *cer3-1* mutants.

In summary, our data exclude *CER3* as the *Arabidopsis* gene At5g02310, which instead encodes PRT6, a ubiquitin ligase of the N-end rule pathway. In confirmation of this result, work by Rowland et al. (unpublished) positively identifies *CER3* as a gene distinct from *PRT6*. We further demonstrate the specificity of PRT6 for proteins with basic amino-terminal residues and show that the *Arabidopsis* N-end rule pathway encompasses at least one additional ubiquitin ligase, which controls the proteolysis of proteins carrying aliphatic hydrophobic amino acids at their amino termini.

Appendix A. Supplementary data

Supplementary data associated with this article can be found, in the online version, at doi:10.1016/j.febslet.2007.06.005.

References

[1] Kerscher, O., Felberbaum, R. and Hochstrasser, M. (2006) Modification of proteins by ubiquitin and ubiquitin-like proteins. Annu. Rev. Cell Dev. Biol. 22, 159–180.

[2] Smalle, J. and Vierstra, R.D. (2004) The ubiquitin 26S proteasome proteolytic pathway. Annu. Rev. Plant Biol. 55, 555–590.

[3] Dreher, K. and Callis, J. (2007) Ubiquitin, hormones and biotic stress in plants. Ann. Bot. 99, 787–822.

[4] Mukhopadhyay, D. and Riezman, H. (2007) Proteasome-independent functions of ubiquitin in endocytosis and signaling. Science 315, 201–205.

[5] Lechner, E., Achard, P., Vansiri, A., Potuschak, T. and Genschik, P. (2006) F-box proteins everywhere. Curr. Opin. Plant Biol. 9, 631–638.

[6] Peters, J.M. (2006) The anaphase promoting complex/cyclosome: a machine designed to destroy. Nat. Rev. Mol. Cell Biol. 7, 644–656.

[7] Kee, Y. and Huibregtse, J.M. (2007) Regulation of catalytic activities of HECT ubiquitin ligases. Biochem. Biophys. Res. Commun. 354, 329–333.

[8] Bachmair, A., Finley, D. and Varshavsky, A. (1986) In vivo half-life of a protein is a function of its amino-terminal residue. Science 234, 179–186.

[9] Varshavsky, A., Turner, G., Du, F. and Xie, Y. (2000) The ubiquitin system and the N-end rule pathway. Biol. Chem. 381, 779–789.

[10] Mogk, A., Schmidt, R. and Bukau, B. (2007) The N-end rule pathway for regulated proteolysis: prokaryotic and eukaryotic strategies. Trends Cell Biol. 17, 165–172.

[11] Hu, R.-G., Sheng, J., Qi, X., Yu, Z., Takahashi, T. and Varshavsky, A. (2005) The N-end rule pathway as a nitric oxide sensor controlling the levels of multiple regulators. Nature 437, 981–986.

[12] Takemoto, D. and Jones, D.A. (2005) Membrane release and destabilization of *Arabidopsis* RIN4 following cleavage by *Pseudomonas syringae* AvrRpt2. Mol. Plant–Microbe Interact. 18, 1258–1268.

[13] Yoshida, S., Ito, M., Callis, J., Nishida, I. and Watanabe, A. (2002) A delayed leaf senescence mutant is defective in arginyl-tRNA:protein arginyltransferase, a component of the N-end rule pathway in *Arabidopsis*. Plant J. 32, 129–137.

[14] Bartel, B., Wünning, I. and Varshavsky, A. (1990) The recognition component of the N-end rule pathway. EMBO J. 9, 3179–3189.

[15] Tasaki, T., Mulder, L.C.F., Iwamatsu, A., Lee, M.J., Davydov, I.V., Varshavsky, A., Muesing, M. and Kwon, Y.T. (2005) A family of mammalian E3 ubiquitin ligases that contain the UBR motif and recognize N-degrons. Mol. Cell. Biol. 25, 7120–7136.

[16] Bachmair, A., Becker, F. and Schell, J. (1993) Use of a reporter transgene to generate Arabidopsis mutants in ubiquitin-dependent protein degradation. Proc. Natl. Acad. Sci. USA 90, 418–421.

[17] Potuschak, T., Stary, S., Schlögelhofer, P., Becker, F., Nejinskaia, V. and Bachmair, A. (1998) *PRT1* of *Arabidopsis thaliana* encodes a component of the plant N-end rule pathway. Proc. Natl. Acad. Sci. USA 95, 7904–7908.

[18] Stary, S., Yin, X.-J., Potuschak, T., Schlögelhofer, P., Nizhynska, V. and Bachmair, A. (2003) PRT1 of *Arabidopsis* is a ubiquitin protein ligase of the plant N-end rule pathway with specificity for aromatic amino-terminal residues. Plant Physiol. 133, 1360–1366.

[19] Hannoufa, A., Negruk, V., Eisner, G. and Lemieux, B. (1996) The *CER3* gene of *Arabidopsis thaliana* is expressed in leaves, stems, roots, flowers and apical meristems. Plant J. 10, 459–467.

[20] Eisner, G., Negruk, V., Hannoufa, A. and Lemieux, B. (1998) Analysis of *Arabidopsis thaliana* transgenic plants transformed with *CER2* and *CER3* genes in sense and antisense orientations. Theor. Appl. Genet. 97, 801–809.

[21] Koornneef, M., Hanhart, C.J. and Thiel, F. (1989) A genetic and phenotypic description of *eceriferum* (*cer*) mutants in *Arabidopsis thaliana*. J. Hered. 80, 118–122.

[22] Kunst, L. and Samuels, A.L. (2003) Biosynthesis and secretion of plant cuticular wax. Prog. Lipid Res. 42, 51–80.

[23] Nawrath, C. (2006) Unraveling the complex network of cuticular structure and function. Curr. Opin. Plant Biol. 9, 281–287.

[24] Sessions, A., Burke, E., Presting, G., Aux, G., McElver, J., Patton, D., Dietrich, B., Ho, P., Bacwaden, J., Ko, C., Clarke, J.D., Cotton, D., Bullis, D., Snell, J., Miguel, T., Hutchison, D., Kimmerly, B., Mitzel, T., Katagiri, F., Glazebrook, J., Law, M. and Goff, S.A. (2002) A high-throughput *Arabidopsis* reverse genetics system. Plant Cell 14, 2985–2994.

[25] Rosso, M.G., Li, Y., Strizhov, N., Reiss, B., Dekker, K. and Weisshaar, B. (2003) An *Arabidopsis thaliana* T-DNA mutagenized population (GABI-Kat) for flanking sequence tag-based reverse genetics. Plant Mol. Biol. 53, 247–259.

[26] Yin, X.-J., Volk, S., Ljung, K., Mehlmer, N., Dolezal, K., Ditengou, F., Hanano, S., Davis, S.J., Schmelzer, E., Sandberg, G., Teige, M., Palme, K., Pickart, C. and Bachmair, A. (in press) Ubiquitin Lys 63 chain forming ligases regulate apical dominance in *Arabidopsis*. Plant Cell.

[27] Schlögelhofer, P., Garzón, M., Kerzendorfer, C., Nizhynska, V. and Bachmair, A. (2006) Expression of the ubiquitin variant ubR48 decreases proteolytic activity in *Arabidopsis* and induces cell death. Planta 223, 684–697.

[28] Kurdyukov, S., Faust, A., Nawrath, C., Bar, S., Voisin, D., Efremova, N., Franke, R., Schreiber, L., Saedler, H., Metraux, J.P. and Yephremov, A. (2006) The epidermis-specific extracellular BODYGUARD controls cuticle development and morphogenesis in Arabidopsis. Plant Cell 18, 321–339.

[29] Altschul, S.F., Gish, W., Miller, W., Myers, E.W. and Lipman, D.J. (1990) Basic local alignment search tool. J. Mol. Biol. 215, 403–410.

[30] Bucher, P., Karplus, K., Moeri, N. and Hofmann, K. (1996) A flexible motif search technique based on generalized profiles. Comput. Chem 20, 3–23.

[31] Edgar, R.C. (2004) MUSCLE: a multiple sequence alignment method with reduced time and space complexity. BMC Bioinformatics 5, 113.

[32] Meinke, D.W., Meinke, L.K., Showalter, T.C., Schissel, A.M., Mueller, L.A. and Tzafrir, I. (2003) A sequence-based map of *Arabidopsis* genes with mutant phenotypes. Plant Physiol. 131, 409–418.

[33] Worley, C.K., Ling, R. and Callis, J. (1998) Engineering in vivo instability of firefly luciferase and *Escherichia coli* β-glucuronidase in higher plants using recognition elements from the ubiquitin pathway. Plant Mol. Biol. 37, 337–347.

[34] Schlögelhofer, P. and Bachmair, A. (2002) A test of fusion protein stability in the plant *Arabidopsis thaliana* reveals degradation signals from ACC synthase and from the plant N-end rule pathway. Plant Cell Rep. 21, 174–179.

[35] Jenks, M.A., Tuttle, H.A., Eigenbrode, S.D. and Feldmann, K.A. (1995) Leaf epicuticular waxes of the *eceriferum* mutants in *Arabidopsis*. Plant Physiol. 108, 369–377.

[36] Jenks, M.A., Tuttle, H.A. and Feldmann, K.A. (1996) Changes in epicuticular waxes on wildtype and *eceriferum* mutants in *Arabidopsis* during development. Phytochemisty 42, 29–34.

[37] Lévy, F., Johnsson, N., Rümenapf, T. and Varshavsky, A. (1996) Using ubiquitin to follow the metabolic fateof a protein. Proc. Natl. Acad. Sci. USA 93, 4907–4912.

[38] Varshavsky, A. (2005) Ubiquitin fusion technique and related methods. Meth. Enzymol. 399, 777–799.

[39] Karsies, A., Hohn, T. and Leclerc, D. (2001) Degradation signals within both terminal domains of the cauliflower mosaic virus capsid protein precursor. Plant J. 27, 335–343.

[40] Baker, R.T. and Varshavsky, A. (1991) Inhibition of the N-end rule pathway in living cells. Proc. Natl. Acad. Sci. USA 88, 1090–1094.

[41] Du, F., Navarro-Garcia, F., Xia, Z., Tasaki, T. and Varshavsky, A. (2002) Pairs of dipeptides synergistically activate the binding of substrate by ubiquitin ligase through dissociation of its autoinhibitory domain. Proc. Natl. Acad. Sci. USA 99, 14110–14115.

[42] Erbse, A., Schmidt, R., Bornemann, T., Schneider-Mergener, J., Mogk, A., Zahn, R., Dougan, D.A. and Bukau, B. (2006) ClpS is an essential component of the N-end rule pathway in *Escherichia coli*. Nature 439, 753–756.

[43] Gil, P., Dewey, E., Friml, J., Zhao, Y., Snowden, K.C., Putterill, J., Palme, K., Estelle, M. and Chory, J. (2001) BIG: calossin-like protein required for polar auxin transport in *Arabidopsis*. Genes Dev. 15, 1985–1997.

[44] Turner, G.C., Du, F. and Varshavsky, A. (2000) Peptides accelerate their uptake by activating a ubiquitin-dependent proteolytic pathway. Nature 405, 579–583.